

# What can Regional Cerebral Blood Flow Measures tell us about the Separation of Normal and Disease Groups?

M.L.J. Scott, N.A. Thacker, A.J. Lacey

Last updated  
03 / 03 / 2003



Imaging Science and Biomedical Engineering,  
School of Cancer and Imaging Sciences,  
University of Manchester, Stopford Building,  
Oxford Road, Manchester M13 9PT, U.K.

# What can Regional Cerebral Blood Flow Measures tell us about the Separation of Normal and Disease Groups?

M.L.J. Scott, N.A. Thacker, A.J. Lacey  
Imaging Science and Biomedical Engineering,  
School of Cancer and Imaging Sciences,  
University of Manchester, Stopford Building,  
Oxford Road, Manchester M13 9PT, U.K.  
paul.bromiley@manchester.ac.uk

## Abstract

This paper describes research exploring the problems associated with interpreting regional blood flow measurements in the brain. We investigate a method for separating normals from those with cerebral diseases, where the disease is caused by, or has resulted in, altered cerebral haemodynamics. Cerebral perfusion maps are divided into 10 vascular territories. The variance scaled mean values from each region are used to determine 10 principle axes of the normal data. We demonstrate that normal variability in these axes is large, but that our technique is capable of detecting measurable perturbations in cerebral haemodynamics. It is also possible to localise disease groups with known vascular change within a portion of the normal space.

## 1 Introduction

Measurement of cerebral blood flow has important actual and potential clinical utility, particularly in diseases such as carotid stenosis, stroke and Alzheimer's dementia. Dynamic T2\* susceptibility contrast enhanced Magnetic Resonance Imaging (DSCE-MRI) can be used to observe the passage of a bolus of Gd-DTPA contrast agent through the brain vasculature and hence effectively image blood flow. We typically acquire 25 contiguous slices over the brain at a temporal resolution of just under 2 seconds for a duration of 80 seconds.

From the contrast concentration time course of the first pass of the bolus through the brain, it is possible to determine the volume of contrast agent in a voxel, as well as the mean time of arrival of the bolus in the voxel [13]. Conventional approaches to perfusion measurement based upon deconvolution of the signal from a voxel by some arterial input function (e.g. [9, 8, 11]) make too many invalid assumptions to provide meaningful estimates of blood flow [14]. These problems centre mainly around an inability to identify genuine input functions due to problems of regional bolus dispersion [1]. However, we have previously shown [12] that parametric image maps of Cerebral Blood Volume (CBV) and Time to Mean (TTM) can be used to calculate the Net Cerebral Blood Flow (NCBF) across a voxel. This approach is based upon the idea of bolus tracking, which defines the local direction and magnitude of velocity of any net flow processes. Such a net flow is implicitly assumed to be negligible in methodologies based upon deconvolution, although we believe it to dominate at the millimetre imaging scales of MRI. The success of our approach fundamentally relies upon the ability to obtain near isotropic voxel dimensions (such as is possible with the PRESTO [4] acquisition), in order that the velocity component of flow can be computed from the TTM maps using spatial differentiation. This technique provides a unique opportunity to determine directional estimates of blood flow at all locations in brain tissue. Such data provides great potential for the analysis of blood flow in disease. Although this is a novel technique, in [13] we demonstrate that normal data agrees with both a physiological model and flow values derived using alternative techniques. However, whatever the physiological meaning of these measures, the true value of the technique can only be found by testing its diagnostic power.

This paper describes an investigation into the utility of using our measures of blood flow in order to separate normal and disease groups. To demonstrate such utility, we must fulfil two criteria. First, that we can quantify change in normals above and beyond that of normal variation and measurement accuracy. Secondly, that normal and disease groups with known cerebral vascular abnormalities will separate in the measurement space. If these criteria are met, the method can be applied to datasets in order to confirm or dispute hypotheses of vascular abnormality.

The approach we have taken is to divide the NCBF and TTM image maps into vascular territories [6]. We have restricted ourselves to one plane of data through the brain at an anatomical level at which it is relatively

Table 1: Subjects groups, numbers, mean age and ranges

Subject Group	Study	Number	Mean Age	Std. Dev	Range
Normal Train	Wellcome	26	73.62	4.76	64-82
Normal Test	RiA	34	72.50	6.41	61-87
Memory Poor	Wellcome	34	73.24	5.23	63-85
Alzheimer's	-	9	61.56	6.15	54-72
Carotid Stenosis	-	5	70.60	-	63-80

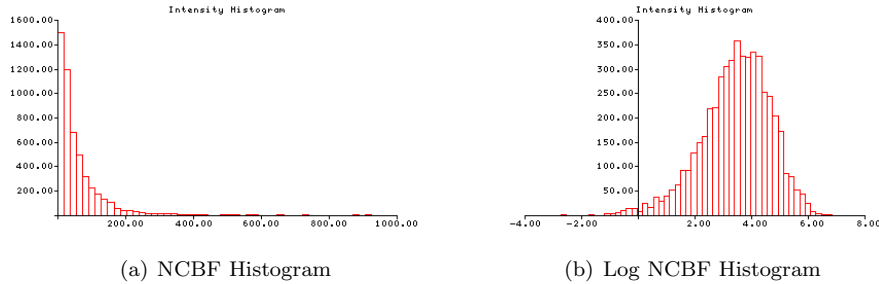


Figure 1: Effect of the Logarithmic transform on NCBF

straightforward to identify vascular territories. This both simplifies the problem of scientific interpretation of results and is consistent with previous publications using deconvolution based techniques [3] which concentrate on only a few slices of the brain. Correlations between the flow values for each region are identified by Principle Components Analysis (PCA), giving us the major modes of variation of the data; a space in which normal and disease groups are expected to separate.

## 2 Methods

### 2.1 Subject Data

Table 1 outlines the groups of subject data, chosen to illustrate the utility of our technique. As well as the normal groups, we have a group of patients with carotid stenoses (all had  $\geq 70\%$  occlusions in at least one carotid artery), who were imaged before and after a carotid endarterectomy (a procedure designed to improve blood flow in arteries) in order to investigate whether we can quantify a change in flow due to the intervention. Patients with Alzheimer's dementia typically show hypoperfusion of parts of the temporal and parietal lobes [5], so this group should separate from the normal groups. Finally, we have a group of patients with amnesic mild cognitive impairment [10] (a possible precursor to Alzheimer's) for which there is a tentative hypothesis that there may be an underlying vascular cause [7].

All subjects underwent a PRESTO scan (TR=28ms, TE=20ms, FA=10°, voxel size = 1.79×1.79×3.5mm). The larger cohorts of subjects have similar mean ages and ranges. The Alzheimer's group has a much lower mean and lower range boundary, typical of the earlier age of onset of this disease. There were too few Carotid Stenosis patients analysed to draw any real conclusions about their mean age, except to say that the age range is comparable to the ages of the other patients in this study.

### 2.2 Statistical Methodology

Interpretation of measurements from a new technique requires an understanding of the statistical characteristics of the data so that genuine changes in observed behaviour can be discriminated from changes due to measurement accuracy. The approach here is to obtain regional averages of voxel measurements for NCBF and TTM and to supply these to algorithms such as Principle Components Analysis (PCA) which can identify systematic correlations.

However, as can be seen from the distribution of NCBF values (Fig. 1(a)) because of the few high flow and many low flow vessels in a slice, means and variances of regional NCBF values are poor summary variables, and certainly not directly suitable for use in PCA. A logarithmic transform is therefore applied to the data in order to make

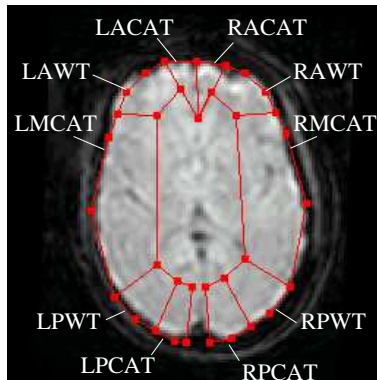


Figure 2: The vascular territories overlaid on a T2\* map. L/R = Left/Right, A/M/PCAT = Anterior/Middle/Posterior Cerebral Arterial Territories, A/PWT = Anterior/Posterior Watershed Territories.

the distribution conform more closely to a Gaussian distribution (Fig. 1(b)). Strictly, PCA requires homogenous measurement errors across the input vector space therefore we need to define an appropriate measurement space for the entire group of subjects. Section 2.4 describes how to achieve this. It is then valid to make use of the mean and standard deviation of the data in this space and more importantly use techniques such as PCA as investigative tools.

The TTM map distributions do approximate a Gaussian distribution, and the numbers again are absolute. However, the data has no fixed origin due to variations between subjects in injection time and bolus passage. In order to compare regions between subjects, we subtract the mean pixel value for the whole slice so that the distribution of values is centred around zero. Note that when looking at disease groups, global delays affecting the whole slice equally will not be detected.

## 2.3 Vascular Regions

As we are interested in detecting localised vascular imbalances in blood flow, it is expedient to divide the brain into vascular territories based on the supply of blood to these regions.

We have devised a method for separating the brain, at the level of the upper border of the third ventricle into 10 classically defined [6] vascular territories. Arterial regions are those directly served by the anterior, middle and posterior cerebral arteries (left and right<sup>1</sup>); the watershed regions (anterior and posterior) are those in between. An active shape model defining control points is fitted to a representative T2\* image using a linear affine transform and the regions are defined according to these points (Fig. 2).

The vascular territories can now be overlaid on the maps of interest (the log(NCBF) or TTM maps) and the mean and standard deviation of the pixel values in each of the 10 regions can be calculated. Note that the number of pixels in the regions varies enormously. The error on the calculation of the mean of the regions is proportional to the square root of the number of pixels ( $N$ ) in the region.

Table 2 gives the means and standard errors for the 10 regions, averaged over 26 normals, for both the log(NCBF) and TTM. As can be seen from the table, there is excellent hemispheric symmetry over the group of normals, particularly for the standard errors. There is no real reason to believe that there should be any difference in the ability to accurately measure the mean between the left and right regions of the brain. Therefore, we can use the average of standard errors of the left and right regions as the scale parameters for our PCA space.

## 2.4 Standardising the Data

For each subject and map type (ie, log(NCBF) or TTM), we have two 10D vectors; one containing the mean values for the 10 regions, the other containing the standard error on the mean of each region, i.e.

$$\mathbf{x}_{i_{mean}} = [x_{RACAT_{mean}i}, x_{RAWY_{mean}i}, \dots, x_{LACAT_{mean}i}] \quad (1)$$

$$\mathbf{x}_{i_{se}} = [x_{RACAT_{se}i}, x_{RAWY_{se}i}, \dots, x_{LACAT_{se}i}] \quad (2)$$

<sup>1</sup>Note that these are the observers left and right, not anatomical.

Table 2: Means and Standard Errors of log(NCBF) and TTM for each region for the normal group. Regions are as given in Fig. 2

Region	log(NCBF)		TTM	
	Avg. Mean	Avg. SE	Avg. Mean	Avg. SE
RACAT	3.05	0.113	0.024	0.123
RAWT	2.64	0.078	0.351	0.098
RMCAT	2.93	0.040	-0.378	0.043
RPWT	2.87	0.076	0.699	0.069
RPCAT	3.02	0.085	0.765	0.084
LPCAT	2.97	0.099	0.768	0.081
LPWT	2.73	0.085	0.729	0.075
LMCAT	2.91	0.042	-0.409	0.040
LAWT	2.73	0.074	0.455	0.086
LACAT	3.22	0.109	-0.046	0.125

where  $i$  is the subject number, RACAT, RAWT etc represent the vascular regions, *mean* and *se* represent whether the vector is composed of the means or the standard errors of the regions.

As explained above, in order to compare the mean pixel values of the different regions using PCA, all the regional values need to have the same statistical scaling i.e. all the regions should have unit variance. To obtain the scale factors, we take the average of the regional standard errors over all of the normal (training) data. The result is a 10D vector of weights

$$\mathbf{w} = \left[ \frac{\sum_{i=1}^I x_{RACAT_{sei}}}{I}, \frac{\sum_{i=1}^I x_{RAWT_{sei}}}{I}, \dots, \frac{\sum_{i=1}^I x_{LACAT_{sei}}}{I} \right] \quad (3)$$

where  $I$  is the total number of the normal (training) patients.

Due to the hemispheric symmetry of the data, we can average the scale factors for the left and right regions and use the same weights for both left and right regions. Here we use only the normal data to create the scale factors because disease processes may bias the weights such that we cannot detect the abnormality. Each element in the  $\mathbf{x}_{i_{mean}}$  vector is scaled by the corresponding weight, to give a vector  $\mathbf{x}_i$ .

## 2.5 Modelling Normal Variation

### 2.5.1 The Covariance Matrix

To transform the data into a form suitable for PCA, we produce a covariance matrix ( $K_x$ ) of the weighted data for the  $N$  Normal subjects

$$K_x = \frac{1}{N-1} \sum_{i=1}^{i=N} (\mathbf{x}_i - \mathbf{m}_{x_n})(\mathbf{x}_i - \mathbf{m}_{x_n})^T \quad (4)$$

where  $\mathbf{m}_{x_n}$  is the 10D vector of the means of the regional mean values for the normals.

The covariance matrix will be 10×10 and shows how the values for the ten regions vary with each other for the corresponding image map (log(NCBF) or TTM).

The covariance matrix allows us to quantify the correlations in flow between all of the vascular regions (see Table 3). The four highest correlations (with a correlation coefficient > 0.75) are illustrated in Fig. 3. The greatest correlations are seen between the left and right anterior watershed territories and the left and right middle cerebral arterial territories. The fact that there is good agreement between symmetrical regions is to be expected and is a sign that the physiological processes involved in NCBF formation are symmetric. There is also a high correlation between the left anterior watershed territory and both adjacent regions (the left anterior and middle cerebral arterial territories). This may be due to the fact that both of the left middle and anterior cerebral arteries (indirectly) feed the watershed region, but may also be due to a misplacement of the boundaries between these regions. With 10 regions, there is a reasonable chance that any one region will be highly correlated with another. However, the

Table 3: Correlation Matrix for weighted Normal NCBF data (correlation of LACAT with itself omitted)

Regions	RACAT	RAWT	RMCAT	RPWT	RPCAT	LPCAT	LPWT	LMCAT	LAWT
RACAT	1.0	-	-	-	-	-	-	-	-
RAWT	0.72	1.0	-	-	-	-	-	-	-
RMCAT	0.53	0.59	1.0	-	-	-	-	-	-
RPWT	0.23	0.57	0.50	1.0	-	-	-	-	-
RPCAT	0.46	0.57	0.63	0.42	1.0	-	-	-	-
LPCAT	0.48	0.57	0.71	0.54	0.69	1.0	-	-	-
LPWT	0.33	0.39	0.44	0.61	0.49	0.63	1.0	-	-
LMCAT	0.60	0.61	0.78	0.61	0.65	0.70	0.54	1.0	-
LAWT	0.60	0.88	0.63	0.62	0.63	0.62	0.37	0.75	1.0
LACAT	0.56	0.76	0.62	0.46	0.56	0.49	0.28	0.66	0.77

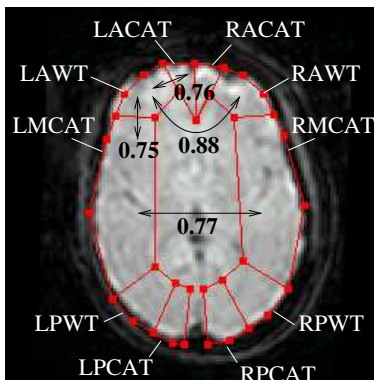


Figure 3: Regions overlaying T2\* map, lines illustrate the correlations between regions as seen in Table 3 and the figures give the correlation coefficients between the regions

fact that the greatest correlations occur between symmetrical territories, where there is no confounding boundary between them, and that these correlations are an average over the whole training set suggests that the correlations represent the true physiology.

### 2.5.2 Principle Components Analysis

Singular Value Decomposition (SVD) is used to perform PCA on the covariance matrix. SVD takes the form

$$A = UWV^T \quad (5)$$

where in our case  $A$  = covariance matrix  $K_x$  ( $10 \times 10$ ),  $W$  is a diagonal matrix, whose values are the 10 eigenvalues ( $\lambda_j$ ) (variance) of the  $K$  matrix.  $U$  and  $V$  are  $10 \times 10$  orthogonal matrices (which in our case happen to be identical), whose columns are the eigenvectors ( $e_j$ ) of the  $K$  matrix.

Interpretation of the results from such an analysis can be aided if we have a good idea of the contribution from statistical noise to the eigenvector space. As our pattern-space has been normalised to the noise process (a change of 1 in measurement is at the level of 1 standard error), we can estimate the contribution to noise in the resulting eigenvector analysis from a Monte-Carlo of a pure 10 dimensional unit Gaussian noise model. The relative magnitudes of the square-root of the eigenvalues for our normal data set and a synthetic Monte-Carlo noise model are shown in Fig. 4. This illustrates a typical result from an eigenvector analysis of an arbitrary data set. Ideally, PCA should result in a reduced representation of the data, however, although there is some evidence that the later eigenvalues in the model are converging on the noise and therefore have no genuine information content, there is no clear separation of the signal and noise components. Some information regarding measurable normal variation is present even at the 10th component which suggests that we do not have a compact model of normal variation with this formulation.

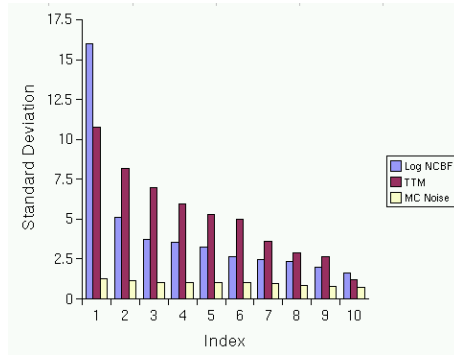


Figure 4: Histogram of standard deviations

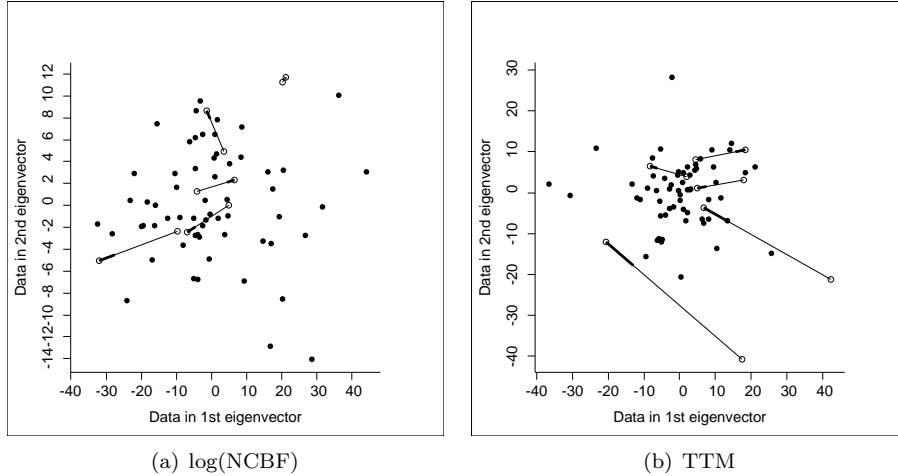


Figure 5: Plot of data in 1st and 2nd eigenvector space for log(NCBF) and TTM data,  $\bullet$  = combined normals,  $\circ$  = carotid stenosis, lines indicate direction of movement after widening of arteries, thick end of line indicates post-operative.

### 3 Results

The eigenvectors are the principle axes of a rotated vector space. We can transform the data into the eigenvector space by calculating the dot product ( $D_{ij}$ ) of the eigenvectors ( $\mathbf{e}_j$ ) and the subject data ( $\mathbf{x}_i$ )

$$D_{ij} = \mathbf{x}_i \mathbf{e}_j \quad (6)$$

where  $j$  is the number of the eigenvector,  $i$  is patient number. As Fig. 4 demonstrates, the first two principle axes (eigenvectors) account for the greatest variation in the normal data and are shown in the following scatterplots.

Plots of the normals and carotid stenosis patients, before and after carotid endarterectomy, for log(NCBF) and TTM are shown in Figs. 5(a) and 5(b). Bearing in mind the eigenvector axes represent the standard error space, there are significant measurable changes post-operatively in both log(NCBF) and TTM for most patients. The direction of change is unimportant here, the main point is that a perturbation in the cerebral blood supply has produced a measurable change. We would not necessarily expect all patients to respond in the same manner, particularly after such a major operation.

Examination of the normals, memory poor and Alzheimer's subjects in the first two components of eigenvector space for both the log(NCBF) (Fig. 6(a)) and TTM (Fig. 6(b)) shows that the data is dominated by normal variation, and that there is no clear separation between any of the groups. Distributions of data in the remaining components of eigenvector space are similar and not reported here. Despite the lack of separation, the Alzheimer's patients do form a distinct cluster at the edge of the boundary of the normal subjects in the log(NCBF) case and have a significantly different mean (at the  $p=0.05$  significance level) from the normals in the 1st eigenvector space ( $p=0.014$ ). Alzheimer's dementia appears to have a systematic vascular component. The Alzheimer's group is younger than the other groups but there is no evidence to suggest that what we are seeing is purely an age-related

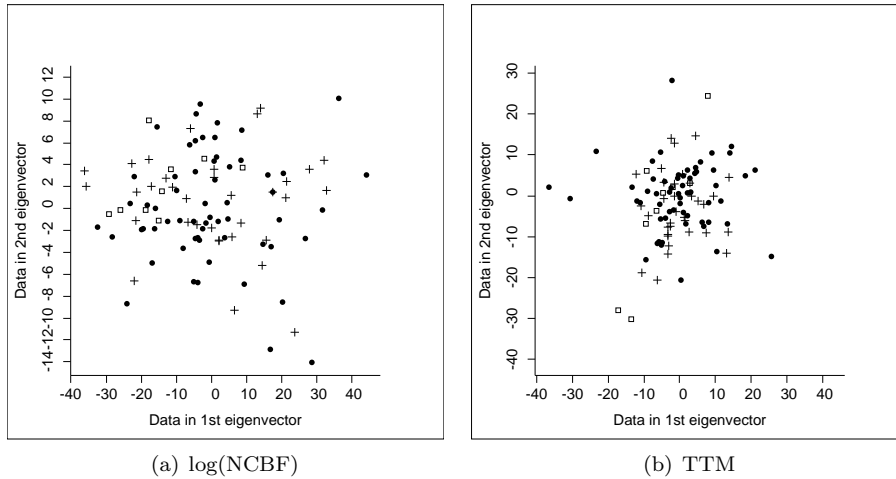


Figure 6: Plot of data in 1st and 2nd eigenvector space for log(NCBF) and TTM data,  $\bullet$  = combined normals,  $\square$  = Alzheimer's,  $+$  = memory poor.

effect, as they do not directly correlate with similar age-matched normals. There appears to be no difference between the normals and memory poor subjects ( $p=0.84$  and  $p=0.58$  for 1st and 2nd eigenvectors).

The mechanisms of the diseases also allows us to hypothesise on the utility of the technique. Carotid stenosis patients have an impediment to flow in one or more of the major brain feeding arteries. We would expect regions supplied by these arteries to be fed slightly later than unimpeded regions, either because the occlusion slows the blood, or because the region is fed by collateral flow. An occlusion would therefore cause a large change in the TTM across the brain. Widening of the arteries would result in a return to normal TTM values. This is indeed shown in Fig. 5(b). By contrast, in terms of vascular disease, Alzheimer's dementia is at the microvascular level [2], where we expect to see localised changes in flow, rather than a consistent alteration in TTM. Again, this is seen in 6(a); there is a consistent trend in the log(NCBF) case and the Alzheimer's patients show no change from normality in the TTM case ( $p=0.13$  and  $p=0.55$  for 1st and 2nd eigenvectors).

## 4 Conclusions

This paper describes a preliminary study in the analysis of regional net flow variables from dynamic susceptibility contrast enhanced MRI. Having taken appropriate account of statistical variability in our data, the results from the normals and carotid stenosis patients suggest that there are significant, measurable differences within the normal group. Subjects with Alzheimer's dementia have group level variations which cause a systematic shift in the group distribution with respect to the normal group but do not cause changes outside the normal observable range. This is an important finding as it suggests that it might not be physiologically possible to exist outside normal flow boundaries and therefore we would never expect to see a clear separation in the log(NCBF) eigenvector space between normal and disease groups.

This technique as it stands is unable to separate disease groups from a normal group. However, we have successfully localised the Alzheimer's patients to a portion of the normal space. In terms of the memory poor individuals, they overlap the normal group well and do not localise in the same manner as the Alzheimer's patients, so we cannot confirm the role of a vascular component in this disorder. The utility of the different flow maps (log(NCBF) or TTM) is dependent upon the disease under investigation. TTM image maps are more likely to be useful when looking at macrovascular disease, log(NCBF) maps will be more useful for small-vessel disease.

Although regional measurements of net flow show promise there are many areas which still require attention. In particular, the large degree of variability of flow patterns in normals could be in part due to an inability to enforce an equivalent physiological state between individuals when scanning. In future work we intend to investigate more rigorous control strategies before and during acquisition. In addition, although this work sets a benchmark for what we can currently achieve, there is still much to be done with regard to analysis of whole volumes of data and also alternative analysis techniques for the identification of correlated changes between groups. Both of these issues are now areas of ongoing research.

Clearly, there are implications regarding the interpretation of identified correlations in this work as these now

correspond to linear correlations between  $\log(\text{NCBF})$  values and not simply NCBF. This is purely a consequence of selecting PCA (effectively a hyperplane fit) as the investigative approach. Our analysis seems to suggest that the correlations between vascular regions are not particularly compactly represented in this representation. However, if there were good reason to think that correlations between regions would be linear in some other domain this may require the development of a purpose designed statistical analysis to replace PCA. Identification of an appropriate representation with which to identify correlated behaviour of flow related variables should be regarded as a fundamental research question.

## Acknowledgements

Work on this paper was supported by a grant from the Wellcome Trust. Thanks to Dr. G. Riding for use of the carotid stenosis patient data, Dr. R.C. Baldwin for the Research into Ageing patients and Prof. A. Jackson and Prof P. Rabbitt for use of the Wellcome Trust data.

## References

- [1] F Calamante, D G Gadian, and A Connelly. Delay and dispersion effects in dynamic susceptibility contrast MRI: Simulations using singular value decomposition. *Magnetic Resonance in Medicine*, 44(3):464–473, Sep 2000.
- [2] E Farkas and P G M Luiten. Cerebral microvascular pathology in aging and Alzheimer’s disease. *Prog. Neurobiol.*, 64:575–611, 2001.
- [3] G J Harris, R F Lewis, A Satlin, C D English, T M Scott, D A Urgelun Todd, and P F Renshaw. Dynamic susceptibility contrast MR imaging of regional cerebral blood volume in alzheimer disease: A promising alternative to nuclear medicine. *Am. J. Neuroradiol.*, 19:1727–1732, 1998.
- [4] G Liu, G Sobering, J Duyn, and C T Moonen. A functional MRI technique combining principles of echo-shifting with a train of observations (PRESTO). *Magn. Reson. Med.*, 30:764–768, 1993.
- [5] K Lobotesis, J D Fenwick, A Phipps, A Ryman, A Swann, C Ballard, I G McKeith, and J T O’Brien. Occipital hypoperfusion on SPECT in dementia with Lewy Bodies but not AD. *Neurol.*, 56:643–649, 2001.
- [6] T B Moller and E Reif. *Pocket Atlas of Cross-Sectional Anatomy CT and MRI*, volume 1; Head, Neck, Spine and Joints. Theime, 1994.
- [7] J H Naish, R C Baldwin, S Jeffries, A S Burns, A Jackson, and C J Taylor. Analysis of cerebral flow in patients with late life depression. In *Proc. MIUA*, volume 6, pages 41–44. BMVA, 2001.
- [8] L Ostergaard, D A Chesler, R M Weisskoff, A G Sorensen, and B R Rosen. Modeling cerebral blood flow and flow heterogeneity from magnetic resonance residue data. *J. Cereb. Blood F. Met.*, 19(6):690–699, Jun 1999.
- [9] L Ostergaard, R M Weisskoff, D A Chesler, and C Gyldensted. High resolution measurement of cerebral blood flow using intravascular tracer bolus passages. Part I: Mathematical approach and statistical analysis. *Magnetic Resonance in Medicine*, 36(5):715–725, Nov 1996.
- [10] R C Petersen, G E Smith, S C Waring, R J Ivnik, E G Tangalos, and E Kokmen. Mild cognitive impairment - clinical characterization and outcome. *Arch. Neurol.*, 56:303–308, March 1999.
- [11] K A Rempp, G Brix, F Wenz, C R Becker, F Guckel, and W J Lorenz. Quantification of regional cerebral blood flow and volume with dynamic susceptibility contrast-enhanced MR imaging. *Radiology*, 193(3):637–641, Dec 1994.
- [12] N A Thacker, M L J Scott, D L Buckley, and A Jackson. A new method for the quantitative calculation of net blood flow using T2\* susceptibility imaging. In *Proc. ISMRM*, Hawaii, 2002.
- [13] N A Thacker, M L J Scott, and A Jackson. Can dynamic susceptibility contrast magnetic resonance imaging perfusion data be analyzed using a model based on directional flow? *J. Magn. Reson. Imaging*, 17(2):241–255, February 2003.
- [14] N A Thacker, X P Zhu, M Nazarpour, C Moonen, and A Jackson. A new approach for the estimation of MTT in bolus passage perfusion techniques. In *Proc. MIUA*, pages 61–64, London, July 2000. BMVA.